Development of experimental methods in electroseismics

Seth Haines, Antoine Guitton, Biondo Biondi Stanford University, Steve Pride, University de Rennes, France*

SUMMARY

The electroseismic method offers the possibility of imaging thin (much smaller than the seismic wavelength) layers in the subsurface. We have collected electroseismic data in the field using a standard seismograph outfitted with electrode pairs rather than geophones, and a sledge hammer and other seismic sources. Removal of coherent source-generated noise is an essential step in the processing of electroseismic data. We accomplish this signal/noise separation using prediction-error filters (PEF's) in an iterative inversion scheme. Using these methods, we image a shallow known target in a controlled setting.

INTRODUCTION

A seismic wave traveling through a fluid-saturated porous material carries with it a charge separation created by the pressure-induced flow of pore fluid. The pore fluid carries a small (but not inconsequential) amount of electric charge relative to the adjacent grains due to the electric double layer (Shaw, 1992) that exists at the grain-fluid boundary. Thus, an electric field (Figure 1) is co-located with a compressional (P) wave propagating through such a material (Pride, 1994). We refer to this field as the "coseismic" field.

The second aspect of the electroseismic response occurs when the P-wave encounters an interface in material properties (elastic, chemical, flow-related, etc). The charge separation in the wave (Figure 2) is disturbed, resulting in what can be approximated as an oscillating electric dipole at the first Fresnel zone (Haartsen and Pride, 1997; Thompson and Gist, 1993). Thus, the resulting electric potential distribution is that of a dipole:

$$V(x,z) = \frac{qd}{4\pi\epsilon_0} \frac{z}{(x^2+z^2)^{3/2}}, \tag{1}$$

where x is the lateral offset, z is the depth to the interface, ϵ_0 is the electrical permittivity, and q is the magnitude of the charges that are separated by distance d. The field of the oscillating dipole (Figure 2b), called the "interface response", can be measured almost immediately at the Earth's surface since the travel-time of electromagnetic radiation is negligible compared with seismic traveltimes ($V_{EM} \gg V_P$).

Both effects can be measured in the field using a standard seismograph equipped with electrode dipoles instead of geophones (Haines et al., 2001; Garambois and Dietrichz, 2001; Thompson and Gist, 1993). The coseismic field contains information only about the properties of the Earth's surface, while the interface response can provide new information about the subsurface. In particular, the interface response is created even for very thin layers, such as a thin fracture zone in otherwise solid rock, or a thin impermeable layer in an aquifer or reservoir. Haines et al. (2001) show that the interface response from a saturated permeable layer 0.6-m thick can be reliably observed. Numerical simulations show that the interface response from a 1-cm embedded impermeable layer is significantly greater than that from an interface between two layers (Stephane Garambois, personal communication 2001). Thus the electroseismic method promises to provide valuable information about important subsurface targets that can not be imaged using other geophysical methods, including information about the location of changes in flow properties.

Electroseismic data collected with a geometry similar to conventional surface seismic data is comprised of both the interface response from subsurface layers and unwanted coseismic energy recorded simultaneously. To enhance the utility of the electroseismic method we must design data processing algorithms to separate the two forms of energy. Transforms (e.g., f-k filtering) have proven ineffective on available data due to the overpowering amplitude of the coseismic noise, and smearing of near-offset coseismic energy across the record. Each shot record eventually will be stacked to produce a single trace corresponding with the subsurface region beneath the shot point. Thus, smeared coseismic energy would be detrimental to the final stack in much the way that inclusion of ground roll or refractions negatively impacts a stacked seismic reflection section.

We describe recent field experiments beyond those of Haines et al. (2001), including increased target complexity and testing of an alternate source. We also present a data processing strategy that separates the signal of interest from the stronger coherent noise using prediction-error filters (PEF's). This signal noise separation is very similar to the reflection seismic problem of multiple attenuation in the angle domain described by Sava and Guitton (2003), and the processing methodologies presented here may be applied to that problem as well.

FIELD METHODS

Haines et al. (2001) present electroseismic experimental methods designed to record the coseismic field and the interface response separately. By imaging a vertical interface with the source and receivers on opposite sides of the target (a two-meter deep trench filled with sand), the interface response can be recorded before the coseismic energy. A second trench was constructed at the site in April, 2002 to add target complexity and realism. Approximately 100 shot records have been recorded at this site with various shot and receiver geometries. Shot gathers are generally stacks of 25 to 100 strikes of a 12 lb sledgehammer on a metal plate located 1 to 4 meters from one side of the trench. We have also tested the use of a shotgun source, firing 400 grain, 12 gauge, blank shells into hand-augered holes. Recording geometries include 24 electrode dipoles ($\sim$1 meter wide) at $\sim$0.7 m spacing located 1 to 4 meters from the other side of the trench. Its distinct polarity reversal and lack of moveout allow us to recognize the interface response on nearly every record. Arrival times and simple amplitude modeling confirm that the observed signal is indeed the interface response. These data provide a unique opportunity for development of a processing sequence to enhance the interface response and remove the coseismic signal.

We remove the energy of the electric power grid using the sinusoid subtraction technique of Butler and Russell (1993) for all harmonics of 60 Hz up to the Nyquist frequency. Bandpass filtering helps to weaken the lower-frequency coseismic noise and the higher-frequency background noise that can obscure weaker arrivals. Application of these pre-processing steps to field data produces results such as that shown in Figure 3.

SIGNAL-NOISE SEPARATION

Electroseismic data (**d**) can be thought of as the sum of two distinct elements- the interface response signal (**s**), the coseismic noise (**n**):

$$\mathbf{d} = \mathbf{s} + \mathbf{n}. \tag{2}$$

In order to separate the interface response from the coseismic noise,

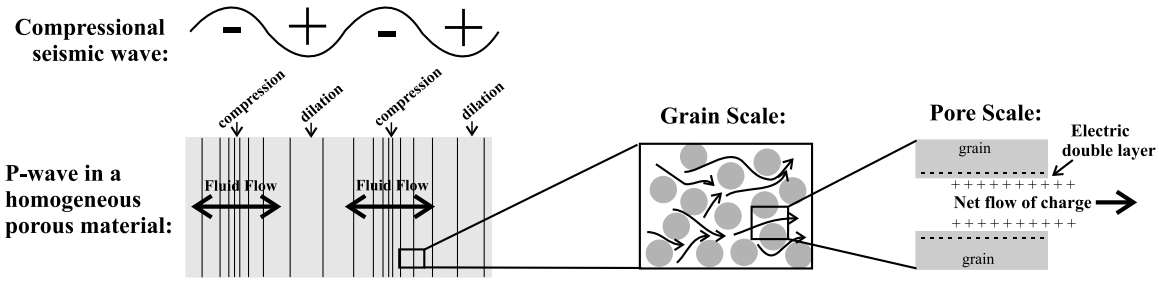

Figure 1: Electroseismic phenomena depend on the charge separation created by streaming currents that flow in response to the pressure gradient of a seismic wave. The electric double layer is responsible for streaming currents at the grain scale.

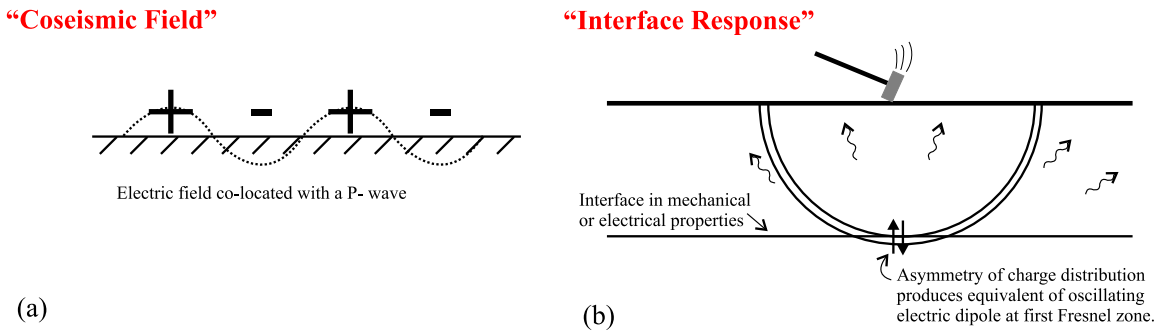

Figure 2: Two types of electroseismic effects that can be measured with electrode dipoles at the Earth's surface: (a) the coseismic field of a P-wave at the surface (represented here by the charge accumulations "+" and "-"), and (b) the interface response created when the P-wave hits an interface at depth.

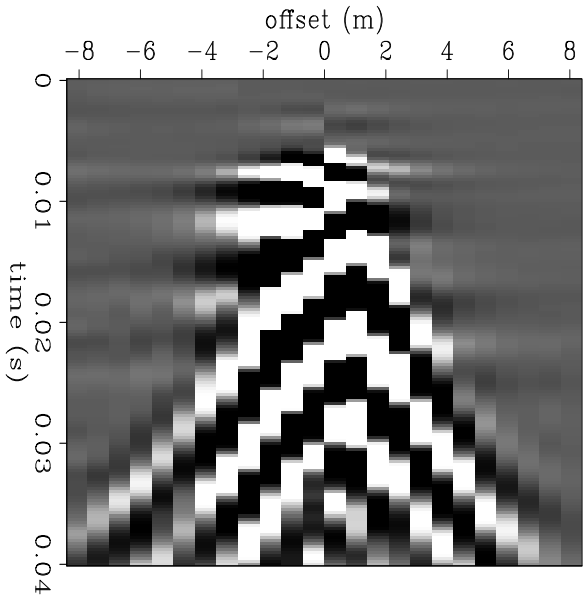

Figure 3: Field data with 60 Hz energy removed and bandpass filter (120-500 Hz) applied. Note horizontal interface response event from first trench at 0.01 seconds and lower-frequency event from second trench at 0.018 seconds . Amplitude asymmetry is somehow caused by shotgun source; a similar record collected with sledgehammer has lower frequency content and symmetric amplitudes. Source and receivers are on the same side of the two trenches, at a distance of two meters from the nearer trench.

we implement a signal-noise separation technique using PEF's **S** and **N** for the signal and noise respectively. Our fitting goals (Soubaras, 1994) are

$$\mathbf{0} \approx \mathbf{N}(\mathbf{s} - \mathbf{d}) \tag{3}$$

and

$$\mathbf{0} \approx \epsilon \mathbf{S}\mathbf{s}, \tag{4}$$

with a least-squares formulation (Guitton et al., 2001) of

$$\hat{\mathbf{s}} = (\mathbf{N}'\mathbf{N} + \epsilon^2 \mathbf{S}'\mathbf{S})^{-1}\mathbf{N}'\mathbf{N}\mathbf{d}. \tag{5}$$

We estimate PEF's **S** and **N** based on windows of the real or synthetic data, and then solve equation 5.

To summarize the processing sequence:

1. Frequency filtering, 60 Hz removal and other pre-processing
2. Determine signal and noise models for estimation of **S** and **N**
3. Estimate PEF's and iteratively solve the inverse problem of equation (5).

TESTING THE SIGNAL/NOISE SEPARATION

Synthetic data

We begin by testing the signal noise separation on synthetic electroseismic data shown in Figure 4a. The horizontal interface response signal in these data is created using equation 1 for the correct amplitude pattern corresponding with the chosen velocity function. The arrival times of interface response and coseismic energy "events" are arbitrarily chosen, as are the relative strengths of the two types of energy. In this example we use non-stationary PEF's in order to better model the entire form of the signal and noise. As a model for estimation of the signal PEF **S** we use a plot of the amplitude pattern predicted for a dipole arrival at every possible travel time, as shown in Figure 4c. **S** is one dimensional, with just one element in time, and ten in the offset direction (size 1,10), so the lack of a waveform in the signal model is not problematic, and adds generality. The noise PEF is estimated using an amplitude balanced version of the coseismic energy present in the original data as shown in Figure 4d, and has size 6 (time) by 4 (offset). Application of the signal-noise processing technique produces the result shown in Figure 4b. The coseismic energy has been almost completely removed, encouraging the application of this technique to field data. One important feature of this technique is the use of a general model (based only on a seismic velocity model) for the estimation of **S**. Thus **S** is designed to look for any interface response energy that may be present, whether or not we have *a priori* knowledge of its arrival time.

Real data

We next test the signal-noise processing approach on field data. These data were collected using the field methods previously described, with the exception that the shot and receivers were both on the same side of the trench, at a distance of 2 meters. Thus these data mimic a traditional subsurface survey geometry, with source and receivers in one line. Data after pre-processing are shown in Figure 5a; note horizontal interface response events at about 0.01 seconds. Signal/noise separation was accomplished using stationary PEF's, so the data were windowed such that positive and negative offsets were processed separately, improving the ability of a single PEF to model the signal or noise in that area. The PEF's were estimated using windows of the real data. A processing result is shown in Figure 5b, with the bulk of the coseismic noise removed. The near-offset parts of the coseismic energy remain, due to the use of a stationary noise PEF that better models the further offsets.

DISCUSSION

Electroseismic data may be collected in the field using a standard seismograph outfitted with electrodes instead of geophones. Signal/noise separation using non-stationary PEF's is an effective approach for removal of coseismic noise in synthetic data. A simplified signal/noise separation approach using stationary PEF's is fairly effective when applied to field data, and suggests that the use of non-stationary PEF's will be more effective. The generality offered by the estimation of the signal PEF on a model of the amplitude pattern expected for the interface response will be valuable when processing field data where the arrival times of interface response events may not be known in advance. We will test the general non-stationary approach on our field data, and on additional data to be collected at various sites, in continuation of this work.

ACKNOWLEDGMENTS

We are grateful to Jerry Harris and Simon Klemperer for guidance throughout this project. The data presented here would not exist without the effort of those who swung the hammer: Nick Martin, Jonathan Franklin, Jordan Muller, T.J. Kiczenski, Morgan Brown, and Stephan Bergbauer. Jim and Carolyn Pride graciously provided the field site, ten dumptrucks full of sand, and some of their outstanding wine. Art Thompson provided some essential electronics, along with important input on data collection. Funding has been provided by the Achievement Rewards for College Scientists Foundation, the Stanford Exploration Project, the Stanford School of Earth Sciences McGee Fund, an AAPG student research grant, and by a GSA student research grant.

REFERENCES

Butler, K. E., and Russell, R. D., 1993, Subtraction of powerline harmonics from geophysical records (short note): Geophysics, **58**, no. 06, 898–903.

Garambois, S., and Dietrichz, M., 2001, Seismoelectric wave conversions in porous media: Field measurements and transfer function analysis: Geophysics, **66**, no. 5, 1417–1430.

Guitton, A., Brown, M., Rickett, J., and Clapp, R., 2001, Multiple attenuation using a t-x pattern-based subtraction method: 71st Ann. Internat. Mtg, Soc. Expl. Geophys., Expanded Abstracts, 1305–1308.

Haartsen, M. W., and Pride, S. R., 1997, Electroseismic waves from point sources in layered media: J. Geophys. Res., **102**, no. B11, 24745–24769.

Haines, S., Pride, S., and Klemperer, S., 2001, Development of experimental methods in electroseismic research, with application to aquifer characterization: Eos Trans. AGU, **82**, no. 47, Abstract GP22A–0268.

Pride, S., 1994, Governing equations for the coupled electromagnetics and acoustics of porous media: Physical Review B, **50**, no. 21, 15678–15696.

Sava, P., and Guitton, A., 2003, Multiple attenuation in the image space: 73rd Annual Internat. Mtg., Soc. Expl. Geophys., Expanded Abstracts, submitted.

Shaw, D., 1992, Introduction to colloid and surface chemistry: Butterworths, 4th edition.

Soubaras, R., 1994, Signal-preserving random noise attenuation by the F-X projection: 64th Ann. Internat. Mtg, Soc. Expl. Geophys., Expanded Abstracts, 1576–1579.

Thompson, A. H., and Gist, G. A., 1993, Geophysical applications of electrokinetic conversion: The Leading Edge, **12**, no. 12, 1169–1173.

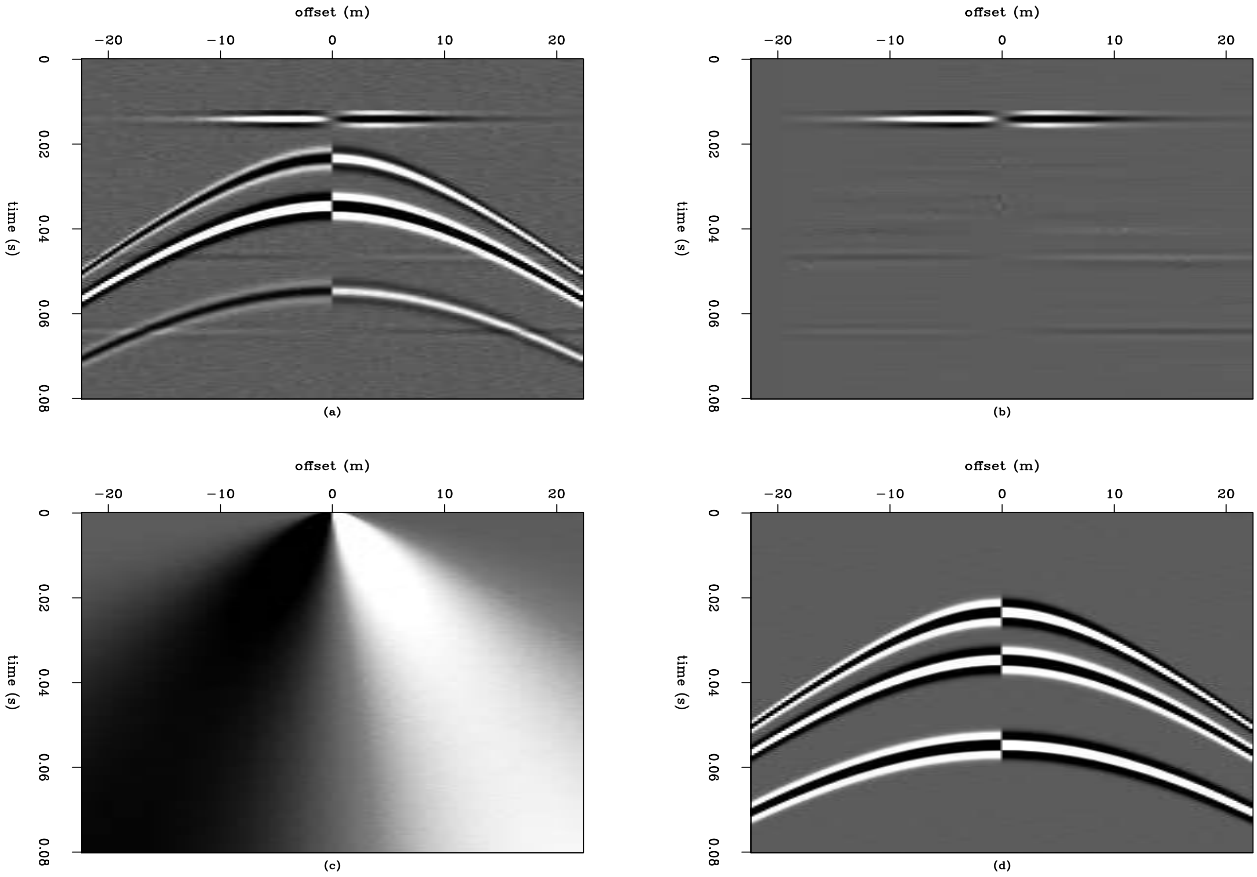

Figure 4: a) Synthetic data, with hyperbolic coseismic noise and horizontal interface response events. b) Result after application of the signal/noise separation technique described. c) Amplitude pattern for dipole field at any given depth, determined using Equation 1, used for estimation of signal PEF. d) Normalized version of coseismic energy, used for estimation of noise PEF.

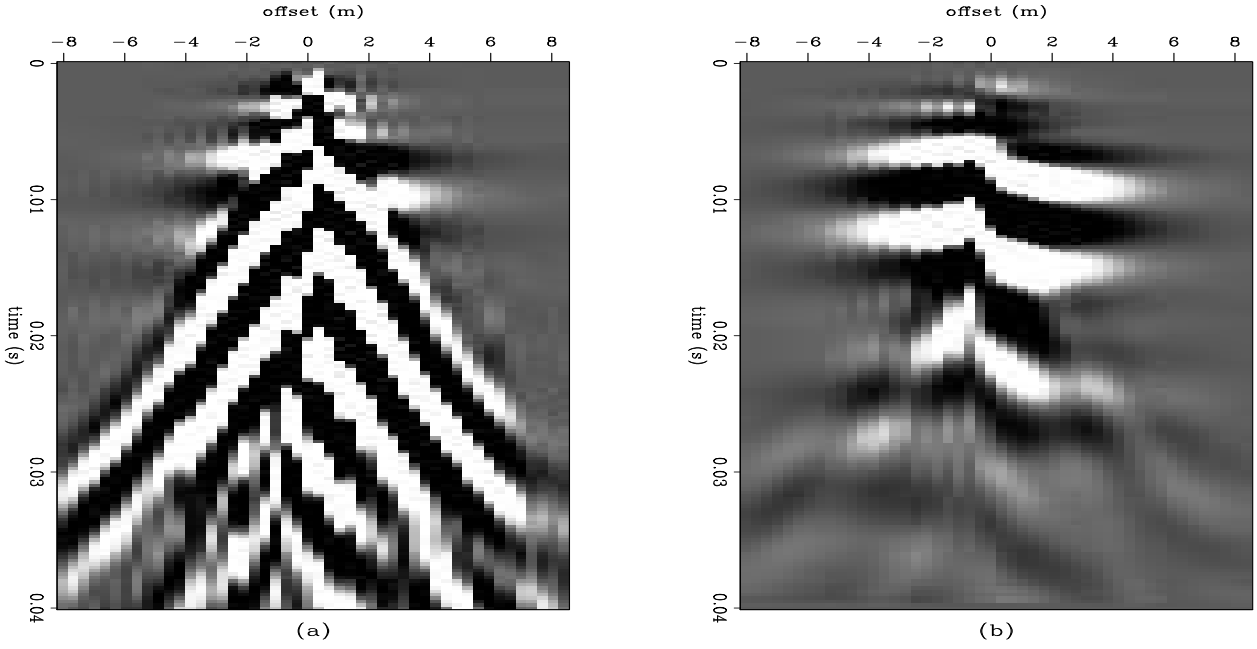

Figure 5: (a) Field data after pre-processing. Source is in the center of electrode receiver array. 48 channel record was achieved by interleaving two 24 channel records. (b) Same data file after signal/noise separation. The majority of the coseismic noise is removed, with the exception of the near offsets where the stationary PEF's used were unable to adequately separate the signal and noise.